Polyoxovanadates: High-Nuclearity Spin Clusters with Interesting Host−Guest Systems and Different Electron Populations. Synthesis, Spin Organization, Magnetochemistry, and Spectroscopic Studies

Achim Müller,*,† Roberta Sessoli,‡ Erich Krickemeyer,† Hartmut Bögge,† Jochen Meyer,† Dante Gatteschi,*,‡ Luca Pardi,§ Jörg Westphal,† Kai Hovemeier,† Ralf Rohlfing,† Joachim Döring,† Frank Hellweg,† Christian Beugholt,† and Marc Schmidtmann†

Fakultät für Chemie, Lehrstuhl für Anorganische Chemie I, Universität Bielefeld, D-33501 Bielefeld, Germany, and Dipartimento di Chimica, Università di Firenze, I-50144 Firenze, Italy

Received March 27, 1997[⊗]

The compounds $Cs_{12}[V^{IV}_{18}O_{42}(H_2O)]\cdot 14H_2O$ (**1a**), $K_{12}[V^{IV}_{18}O_{42}(H_2O)]\cdot 16H_2O$ (**1b**), $Rb_{12}[V^{IV}_{18}O_{42}(H_2O)]\cdot 19H_2O$ (**1c**), $K_9[H_3V^{IV}_{18}O_{42}(H_2O)]\cdot 14H_2O\cdot 4N_2H_4$ (**1d**), $K_{11}[H_2V^{IV}_{18}O_{42}(Cl)]\cdot 13H_2O\cdot 2N_2H_4$ (**2a**), $K_9[H_4V^{IV}_{18}O_{42}(Br)]\cdot 14H_2O\cdot 4N_2H_4$ (**2b**), $K_9[H_4V^{IV}_{18}O_{42}(I)]\cdot 14H_2O\cdot 4N_2H_4$ (**2c**), $K_{10}[H_3V^{IV}_{18}O_{42}(Br)]\cdot 13H_2O\cdot 0.5N_2H_4$ (**2d**), $K_9[H_4V^{IV}_{18}O_{42}(NO_2)]\cdot 14\ H_2O\cdot 4N_2H_4$ (**3**), $Cs_{11}[H_2V^{IV}_{18}O_{42}(SH)]\cdot 12H_2O$ (**4**), $K_{10}[HV^{IV}_{16}V^{V}_{2}O_{42}(Cl)]\cdot 16H_2O$ (**5a**), $Cs_9[H_2V^{IV}_{16}V^{V}_{2}O_{42}(Br)]\cdot 12H_2O$ (**5b**), $K_{10}[HV^{IV}_{16}V^{V}_{2}O_{42}(Br)]\cdot 16H_2O$ (**5c**), $Cs_9[H_2V^{IV}_{16}V^{V}_{2}O_{42}(I)]\cdot 12H_2O$ (**5d**), $K_{10}[HV^{IV}_{16}V^{V}_{2}O_{42}(I)]\cdot 16H_2O$ (**5e**), $K_{10}[HV^{IV}_{16}V^{V}_{2}O_{42}(HCOO)]\cdot 15H_2O$ (**6**), $(NEt_4)_5[V^{IV}_{10}V^{V}_{8}O_{42}(I)]$ (**7**), and $Na_6[H_7V^{IV}_{16}V^{V}_{2}O_{42}(VO_4)]\cdot 21H_2O$ (**8**) have been characterized by elemental analyses, redox titrations, IR and EPR spectroscopy, and magnetic susceptibility measurements, as well as by single crystal X-ray structure analyses. The anions contain—as a common structural feature—an approximately spherical $\{V_{18}O_{42}\}$ shell, which can act as a unique host system for neutral and anionic guests. Remarkably, the electron population of these clusters can—depending on the specific reaction conditions—be varied in a wide range between 10 and 18 3d electrons without changing the overall structure. The related magnetic properties in connection with the phenomenon of electron-dependent spin organization on a spherical cluster shell have been discussed in detail.

Introduction

Vanadium in its higher oxidation states tends to form polynuclear, anionic metal−oxygen clusters with an extraordinary variety of the relevant topology and electronic structures.[1] This variety can be attributed to the multitude of possibilities to link basic building blocks which correspond to $\{V^{n+}O_x\}$ polyhedra ($x = 4, 5, 6$) like tetrahedra, tetragonal pyramids, or octahedra. The resulting structures range from quite compact forms, like in the case of $V_{10}O_{28}^{6-}$, to open ribbon-, basket-, shell-, and cagelike host systems,[2] suitable for the uptake of neutral[3−6]as well as ionic guests.[7−16] In addition, also two-dimensional layered materials[17,18] as well as three-dimensional host structures[19] have been described in recent years.

Apart from their interesting structural variety, polyoxovanadates show remarkable, facile redox processes so that the species can exist with quite different electron populations. The corresponding clusters are of special interest for different aspects of bioinorganic and magnetochemistry but also for research in homogeneous and heterogeneous catalysis.[20]

Whereas it is usually unproblematical today to determine the basic geometric structure even of rather complex polyvanadates, the determination of the electronic structure can be very complicated. This refers in particular to the problem of distinguishing for instance between cluster shells of the type $V^{IV}_{m}V^{V}_{n}$ and $V^{IV}_{m-x}V^{V}_{n+x}$ for large m and n and small values of x mainly if the calculation of the charge on the cluster anion is not possible due to difficulties in determining the degree of protonation *and* the number of cations with sufficient accuracy. To avoid errors, application of different physical apart from analytical methods is often indispensable. In order to confirm the obtained results the knowledge of magnetic susceptibility and EPR data is of utmost importance. In this paper, compounds with structurally equivalent $\{V_{18}O_{42}\}$ shells but remarkably

† University of Bielefeld.
‡ University of Florence.
§ National High Magnetic Field Laboratory, Tallahassee, FL.
⊗ Abstract published in *Advance ACS Abstracts,* October 1, 1997.

(1) Pope, M. T.; Müller A. *Angew. Chem., Int. Ed. Engl.* **1991**, *30*, 34.
(2) Klemperer, W. G.; Marquart, T. A.; Yagi, O. M. *Angew. Chem., Int. Ed. Engl*. **1992**, *31*, 49.
(3) Johnson, G. K.; Schlemper, E. O. *J. Am. Chem. Soc.* **1978**, *100*, 3645.
(4) Johnson, G. K. Ph.D. Thesis, University of Missouri—Columbia, 1977; *Diss. Abst.* **1978**, *38B*, 4801. See also: Pope, M. T. *Heteropoly and Isopoly Oxometalates*; Springer: Berlin, 1983; pp 38−39.
(5) Day, V. W.; Klemperer, W. G.; Yagi, O. M. *J. Am. Chem. Soc.* **1989**, *111*, 5959.
(6) Khan, M. I.; Zubieta, J. *Angew. Chem., Int. Ed. Engl.* **1994**, *33*, 760.
(7) Priebsch, W.; Rehder, D.; von Oeynhausen, M. *Chem. Ber*. **1991**, *124*, 761.
(8) Huan, G.; Jacobsen, A. J.; Day, V. W. *Angew. Chem., Int. Ed. Engl.* **1991**, *30*, 422.
(9) Heinrich, D. D.; Folting, K.; Streib, W. E.; Huffman, J. C.; Christou, G. *J. Chem. Soc., Chem. Commun.* **1989**, 1411.
(10) Chen, Q.; Liu, S.; Zubieta, J. *Inorg. Chem*. **1989**, *28*, 4433.
(11) Müller, A.; Penk, M.; Rohlfing, R.; Krickemeyer, E.; Döring, J. *Angew. Chem., Int. Ed. Engl.* **1990**, *29*, 926.
(12) Müller, A.; Krickemeyer, E.; Penk, M.; Rohlfing, R.; Armatage, A.; Bögge, H. *Angew. Chem., Int. Ed. Engl.* **1991**, *30*, 1674.
(13) Müller, A.; Hovemeier, K.; Rohlfing, R. *Angew. Chem., Int. Ed. Engl.* **1992**, *31*, 1192.
(14) Müller, A.; Rohlfing, R.; Krickemeyer, E.; Bögge, H. *Angew. Chem., Int. Ed. Engl*. **1993**, *32*, 909.
(15) Müller, A.; Döring, J.; Bögge, H.; Krickemeyer, E. *Chimia* **1988**, *42*, 300.
(16) Salta, J.; Chen, Q.; Chang, Y. D.; Zubieta, J. *Angew. Chem., Int. Ed. Engl.* **1994**, *33*, 757.
(17) Khan, M. I.; Lee, Y. S.; O'Connor, C. J.; Haushalter, R. C.; Zubieta, J. *J. Am. Chem. Soc.* **1994**, *116*, 4525.
(18) Haushalter, R. C.; Wang, Z.; Thompson, M. E.; Zubieta, J.; O'Connor, C. J. *Inorg. Chem.* **1993**, *32*, 3966.
(19) Soghomonian, V.; Chen, Q.; Haushalter, R. C.; Zubieta, J. *Angew. Chem., Int. Ed. Engl.* **1993**, *32*, 610.
(20) Rehder, D. *Angew. Chem., Int. Ed. Engl.* **1991**, *30*, 148.

S0020-1669(97)00364-9 CCC: $14.00

different electron populations and with unusual host−guest chemistry will be reported. The related magnetic properties are discussed in detail. For the magnetochemist, these compounds are of particular interest since they belong to the class of high-nuclearity spin clusters.

Experimental Section

(a) Syntheses. All manipulations for the syntheses of **1a**−**c**, **2d**, and **4** were carried out under an argon atmosphere. Doubly-destilled water was used for all reactions which was additionally degassed (oxygen free) in the case of **1a**−**c**, **2d**, and **4**. All substances (with the exception of **1c**) were stored under an argon atmosphere over $CaCl_2$. The crystals of **1d**−**3** slowly lose N_2H_4.

1a. 15.0 g (95 mmol) CsOH (95%) and 5.7 g (22.5 mmol) of $VOSO_4 \cdot 5\ H_2O$ are successively dissolved in 70 mL H_2O in a 100 mL round-bottomed flask at 50 - 60 °C. After stirring the solution for some minutes at this temperature, the resulting dark-brown solution is cooled down to room temperature in the closed flask and allowed to stand for crystallization for 3−4 d. The supernatant mother liquid is completely decanted and the blackish-brown crystals of **1a** are separated from the brown less-crystalline precipitate by slurrying with 50% aqueous 2-propanol followed by decantation. The crystals are washed with 2-propanol and afterward dried in an argon stream. Yield: 3.3 g (76% based on V). Anal. Calcd for $H_{30}Cs_{12}O_{57}V_{18}$: Cs, 46.18; H_2O, 7.82. Found: Cs, 45.6; H_2O, 7.4.

1b. (See also refs 3 and 4.) Solutions of 11.4 g (45 mmol) of $VOSO_4 \cdot 5H_2O$ in 25 mL of H_2O and of 19.4 g (346 mmol) of KOH in 50 mL of H_2O are successively added to 100 mL of 4.5% H_2SO_4. The resulting dark-brown solution is heated to 60−70 °C for 5 min and then cooled to room temperature and allowed to stand in a closed flask for crystallization for 1 d. The obtained brown microcrystalline crude product of **1b** is separated from the solution by decantation and again redissolved in 200 mL of a 1.2% aqueous solution of KOH at 60−70 °C. After being cooled to room temperature, the solution is again allowed to stand in a closed flask for crystallization for 1 d. The supernatant mother liquid is completely decanted, and the blackish-brown crystals of **1b** are washed successively with 50% aqueous 2-propanol and 2-propanol and afterward dried in an argon stream. Yield: 2.95 g (50% based on V). Anal. Calcd for $H_{34}K_{12}O_{59}V_{18}$: K, 19.85; H_2O, 12.95. Found: K, 21.0; H_2O, 12.0.

1c. A 15 mL volume of a 0.5 M aqueous solution of $VO(ClO_4)_2$ (7.5 mmol) is added to a solution of 4.1 g (20 mmol) of 50% RbOH in 20 mL of H_2O in a 100 mL round-bottomed flask while stirring. After being stirred for 2 h at 90 °C, the solution is cooled to room temperature and allowed to stand in the closed flask for crystallization. After 12 h, crystals of $RbClO_4$ are filtered off, and blackish-brown crystals of **1c** were isolated from the filtrate after 1 day. The crystals are not stable outside the mother liquor and decompose by losing crystal water. Yield: 0.45 g (36% based on V). Anal. Calcd for $H_{40}O_{62}Rb_{12}V_{18}$: Rb, 34.48; H_2O, 12.11. Found: Rb, 36.2; H_2O, 12.0.

1d. A solution of 4.0 g (1.7 mmol) of **1b** and 8 mL (165 mmol) of N_2H_5OH (100%) in 100 mL of H_2O is kept for 2 h at 90 °C in an Erlenmeyer flask (covered with a watch glass) without stirring. After being cooled to room temperature, the dark-brown solution is allowed to stand in the closed flask for crystallization for 1 d. The supernatant mother liquid is completely decanted, and the blackish-brown crystals are washed successively with 50% aqueous 2-propanol and 2-propanol and afterward dried in an argon stream. Besides crystals of **1d** for which the X-ray structure analysis was done, crystals with the same spectroscopic properties but different powder diffraction diagram were obtained.

2a. A solution of 1.0 g (0.42 mmol) of **1b**, 2 mL (41.2 mmol) of N_2H_5OH (100%), and 0.1 g (1.3 mmol) of KCl in 50 mL of H_2O is kept for 4 h at 90 °C in an Erlenmeyer flask (covered with a watch glass) without stirring. After being cooled to room temperature, the dark-brown solution is allowed to stand in the closed flask for crystallization for 1−2 d. The supernatant mother liquid is completely decanted, and the blackish-brown crystals of **2a** are washed successively with 50% aqueous 2-propanol and 2-propanol and afterward dried in an argon stream. Yield: 0.3 g (30% based on V). Anal. Calcd for $H_{36}ClK_{11}N_4O_{55}V_{18}$: Cl, 1.50; K, 18.27; N, 2.38. Found: Cl, 1.3; K, 19.1; N, 2.39.

2b,c. The syntheses are analogous to that of **2a** using 0.1 g (0.8 mmol) of KBr (**2b**) and 0.1 g (0.6 mmol) of KI (**2c**), respectively, instead of KCl. Yield: **2b**, 0.6 g (59%); **2c**, 0.7 g (68%; all values based on V). **2b**: Anal. Calcd for $H_{48}BrK_9N_8O_{56}V_{18}$: Br, 3.32; K, 14.63; N, 4.66. Found: Br, 3.4; K, 14.5; N, 4.14. **2c**: Anal. Calcd for $H_{48}IK_9O_{56}N_8V_{18}$: I, 5.18; K, 14.35; N, 4.57. Found: I, 5.3; K, 14.4; N, 4.14.

2d. A 27.6 g (200 mmol) amount of KVO_3 and 2.88 mL (59.3 mmol) of N_2H_5OH (100%) are successively dissolved in 400 mL of H_2O at 80 °C in a 500 mL round-bottom flask (vigorous evolution of N_2!), and the solution is refluxed for 0.5 h. Afterward, 9.05 mL of HBr (48%) is added to the resulting dark-brown solution which is again refluxed for 0.5 h. After the solution is cooled to room temperature, blackish-brown crystals of **5c** are obtained within 16 h. To the supernatant mother liquid 36.5 mL (752 mmol) of N_2H_5OH (100%) is added, and the crystals are redissolved in the mother liquid at 100 °C and refluxed for 2 h. After being cooled to room temperature the dark-brown solution is allowed to stand in the closed flask for crystallization for 1 d. The supernatant mother liquid is completely decanted, and the blackish-brown crystals of **2d** are separated from the brown less-crystalline precipitate by slurrying with 50% aqueous 2-propanol followed by decantation. Then the crystals are washed with 2-propanol and afterward dried in an argon stream. Yield: 22 g (86% based on V). Anal. Calcd for $H_{31}BrNK_{10}O_{55}V_{18}$: Br, 3.45; K, 16.91; N, 0.61. Found: Br, 3.6; K, 15.8; N, 0.88.

3. A solution of 8.0 g (3.4 mmol) of **1b**, 0.8 g (9.4 mmol) of KNO_2, and 16 mL (330 mmol) of N_2H_5OH (100%) in 400 mL of H_2O is kept for 2 h without stirring at 95 °C in a 500 mL round-bottom flask (oil bath; flask covered with a watch glass). Afterward, the resulting dark-brown solution is slowly cooled to room temperature within 3 h and allowed to crystallize in the closed flask for 5 d. The supernatant mother liquid is completely decanted, and the blackish-brown crystals of **3** are successively washed with 50% aqueous 2-propanol and 2-propanol and afterward dried in an argon stream. Yield: 4.0 g (50% based on V). Anal. Calcd for $H_{48}K_9N_9O_{58}V_{18}$: K, 14.84; N, 5.32. Found: K, 15.4; N, 5.24.

4. An 11.6 g (50 mmol) amount of $CsVO_3$ is dissolved in 250 mL of H_2O at 90 °C in a 500 mL round-bottom flask, and the pH of the solution is adjusted to 8.2 with CsOH. Afterward a moderate stream (10 L/h) of H_2S gas is passed through the solution for ca. 10 min. The obtained dark-brown solution is allowed to stand for 2 h further at 90 °C, cooled to room temperature, and stored in the closed flask for crystallization for 1 d. The supernatant mother liquid is completely decanted, and the blackish-brown crystals of **4** are washed with 50% aqueous 2-propanol, 2-propanol, CS_2 (for the removal of the precipitated sulfur), and again with 2-propanol and dried in an argon stream. Yield: 6.4 g (59% based on V). Anal. Calcd for $H_{27}Cs_{11}O_{54}SV_{18}$: Cs, 44.27; S, 0.97; H_2O 6.54. Found: Cs, 44.8; S, 1.0; H_2O, 5.6.

5a,c,e. (See also ref 11.). A 360 μL (7.4 mmol) amount of N_2H_5OH (100%) is dissolved in a solution of 3.45 g (25 mmol) of KVO_3 in 50 mL of H_2O at 90 °C, and the solution is allowed to stand at this temperature without stirring for 1 h in an Erlenmeyer flask (covered with a watch glass). Afterward, 0.83 mL of 37% HCl and 0.07 mL of 100% N_2H_5OH (**5a**), 1.13 mL of 48% HBr (**5c**), or 1.34 mL of 57% HI (**5e**), respectively, are added to the resulting dark-brown solution. The solution is allowed to stand for 4 h at 90 °C without stirring, cooled to room temperature, and stored in the closed flask for crystallization for 1 d. The supernatant mother liquid is completely decanted, and the blackish-brown crystals are washed successively with 50% aqueous 2-propanol and 2-propanol and afterward dried in an argon stream. Yield: **5a**, 1.3 g (41%); **5c**, 2.4 g (74%); **5e**, 2.6 g (78%; all values based on V). **5a**: Anal. Calcd for $H_{33}ClK_{10}O_{58}V_{18}$: Cl, 1.54; K, 16.97; H_2O, 12.51. Found: Cl, 1.6; K, 16.1; H_2O, 12.6. **5c**: Anal. Calcd for $H_{33}BrK_{10}O_{58}V_{18}$: Br, 3.40; K, 16.65; H_2O, 12.27. Found: Br, 3.7; K, 15.9; H_2O, 12.4. **5e**: Anal. Calcd for $H_{33}IK_{10}O_{58}V_{18}$: I, 5.30; K, 16.32; H_2O, 12.03. Found: I, 5.8; K, 15.8; H_2O, 12.1.

5b,d. (See also ref 11.). A 180 μL (3.7 mmol) amount of N_2H_5OH (100%) is dissolved in a solution of 1.16 g (5 mmol) of $CsVO_3$ in 100 mL of H_2O at 90 °C, and the solution is allowed to stand at this

temperature without stirring for 1 h in an Erlenmeyer flask (covered with a watch glass). Afterward, the pH value of the resulting dark-brown solution is adjusted by dropwise addition of 48% HBr (**5b**) or 57% HI (**5d**), respectively every 15 min to 7.9−8.0 until it remains constant (ca. 1−1.5 h). After the reaction mixture was kept at 90 °C for 1.5 h, it is slowly cooled to room temperature and allowed to stand in the closed flask for crystallization for 1 d. The supernatant mother liquid is completely decanted, and the blackish-brown crystals are washed successively with 50% aqueous 2-propanol and 2-propanol and afterward dried in an argon stream. Yield: **5b**, 0.2 g (23%); **5d**, 0.2 g (23%; all values based on V). **5b**: Anal. Calcd for $H_{26}BrCs_9O_{54}V_{18}$: Br, 2.59; Cs, 38.80; H_2O, 7.01. Found: Br, 2.9; Cs, 37.9; H_2O, 7.0. **5d**: Anal. Calcd for $H_{26}Cs_9IO_{54}V_{18}$: Cs, 38.21; I, 4.05; H_2O, 6.91. Found: Cs, 37.7; I, 4.3; H_2O, 6.8.

6. A 360 μL (7.4 mmol) amount of N_2H_5OH (100%) is dissolved in a solution of 3.45 g (25 mmol) of KVO_3 in 50 mL of H_2O at 90 °C, and the solution is allowed to stand at this temperature without stirring for 1 h in an Erlenmeyer flask (covered with a watch glass). The pH value of the resulting dark-brown solution is adjusted with 50% HCOOH to ca. 7.8, which is then maintained. During a period of 2.5−3 h additional amounts of HCOOH are added every 15 min to keep the pH value constant. After 2.5 h, the reaction mixture (still kept at 90 °C) is slowly cooled to room temperature and allowed to stand in the closed flask for crystallization for 1 d. The obtained black crystals of **6** are filtered off and dried on filter paper in air. Yield: 2.1 g (66% based on V). Anal. Calcd for $CH_{32}K_{10}O_{59}V_{18}$: C, 0.52; K, 17.03; H_2O, 11.77. Found: C, 0.49; K, 16.6; H_2O, 10.7.

7. A 1.65 g (0.72 mmol) amount of freshly prepared $(NH_4)_8[V_{18}O_{42}(SO_4)]\cdot 25H_2O$[15] is added to a solution of 4.0 g (15.6 mmol) of $(NEt_4)I$ in 250 mL of H_2O. The reaction mixture is allowed to stand at 85 °C in an Erlenmeyer flask (covered with a watch glass) for 6 h without stirring. After the solution was cooled to room temperature, black crystals of **7** precipitate from the reaction mixture within 2−3 d. The obtained crystals are filtered off, washed with H_2O, and dried on filter paper in air. Yield: 0.9 g (53% based on V). Anal. Calcd for $C_{40}H_{100}IN_5O_{42}V_{18}$: C, 20.30; H, 4.26; N, 2.96. Found: C, 20.47; H, 4.18; N, 3.04.

8. See ref 15.

(b) Chemical Analyses. Sodium and potassium were determined by FES (Pye Unicam SP 1900 spectrophotometer); cesium, iodine, and rubidium, by ICP-MS (Plasma Quad 2; VG elemental). The analyses of Cl^- and Br^- were carried out by using the method of ion chromatography (Dionex-QIC analyzer with a Shimadzu C-R3A-chromatograph integrator); HS^- was oxidized to SO_4^{2-} (alkaline H_2O_2 solution) and also determined by ion chromatography. The analyses of carbon, hydrogen, and nitrogen were carried out at the analytical department of the University of Bielefeld using a Perkin-Elmer 420 element analyzer. The content of crystal water was determined thermogravimetrically with a Linseis L 81 instrument. The determination of the number of V^{IV} centers was carried out by potentiometric titration with 0.1 N $KMnO_4$ using a Mettler DL 40 memotitrator (Pt/calomel electrode).

(c) Crystal Structure Analyses. The structures were determined from single-crystal X-ray diffraction data (Siemens R3m/V four-circle diffractometer). Crystal data and details concerning the intensity data collections and stucture refinements are given in Table 1. Unit cell parameters were obtained by least-squares refinement of the angular settings of high-angle reflections. An empirical absorption correction was applied for all compounds (except for **1c** and **8**) and the data corrected for Lorentz and polarization effects. All structures were solved by direct methods (SHELXTL program package[21]). Final least-squares refinements converged to values given in Table 1. Atomic scattering factors for all atoms were taken from standard sources whereby anomalous dispersion corrections were applied to all atoms.[22] Positional parameters of three typical compounds belonging to three different classes (see below) are given in Tables 2−4.

(d) IR Spectroscopy. IR spectra were measured using a Mattson Polaris FT-IR spectrometer (KBr pellets) as well as a Bruker IFS 66/FRA 106 instrument.

(e) EPR Spectroscopy and Magnetic Susceptibility Measurements. The magnetic susceptibility was measured using a Metronique Ingenierie SQUID magnetometer with an applied field of 10 KOe whereby the diamagnetic contribution of the compounds was estimated using Pascal's constants. The EPR spectra were recorded on polycrystalline powders at X-band frequency on a Varian E-9 spectrometer at different temperatures.

Results and Discussion

The chemistry of reduced polyoxovanadates in aqueous solution is characterized by the high formation tendency of species with cagelike structures which can act as host systems for neutral and anionic guests.[3,11−16] The shape and size of the host systems are often determined by the kind of the encapsulated guest. A template-induced formation of some of these clusters has been proposed though in some cases also a nonspecific container function of the cluster shell can be assumed.[23] A typical example for host systems for small guests are polyvanadate cluster anions with an approximately spherical $\{V_{18}O_{42}\}$ shell. In recent years we succeeded in isolating a large number of compounds containing this type of shell (Tables 1−5): $Cs_{12}[V^{IV}{}_{18}O_{42}(H_2O)]\cdot 14H_2O$ (**1a**); $K_{12}[V^{IV}{}_{18}O_{42}(H_2O)]\cdot 16H_2O$ (**1b**); $Rb_{12}[V^{IV}{}_{18}O_{42}(H_2O)]\cdot 19H_2O$ (**1c**); $K_9[H_3V^{IV}{}_{18}O_{42}(H_2O)]\cdot 14H_2O\cdot 4N_2H_4$ (**1d**); $K_{11}[H_2V^{IV}{}_{18}O_{42}(Cl)]\cdot 13H_2O\cdot 2N_2H_4$ (**2a**); $K_9[H_4V^{IV}{}_{18}O_{42}(Br)]\cdot 14H_2O\cdot 4N_2H_4$ (**2b**); $K_9[H_4V^{IV}{}_{18}O_{42}(I)]\cdot 14H_2O\cdot 4N_2H_4$ (**2c**); $K_{10}[H_3V^{IV}{}_{18}O_{42}(Br)]\cdot 13H_2O\cdot 0.5N_2H_4$ (**2d**); $K_9[H_4V^{IV}{}_{18}O_{42}(NO_2)]\cdot 14H_2O\cdot 4N_2H_4$ (**3**); $Cs_{11}[H_2V^{IV}{}_{18}O_{42}(SH)]\cdot 12H_2O$ (**4**) (regarding the formula see text); $K_{10}[HV^{IV}{}_{16}V^{V}{}_2O_{42}(Cl)]\cdot 16\ H_2O$ (**5a**); $Cs_9[H_2V^{IV}{}_{16}V^{V}{}_2O_{42}(Br)]\cdot 12H_2O$ (**5b**); $K_{10}[HV^{IV}{}_{16}V^{V}{}_2O_{42}(Br)]\cdot 16H_2O$ (**5c**); $Cs_9[H_2V^{IV}{}_{16}V^{V}{}_2O_{42}(I)]\cdot 12H_2O$ (**5d**); $K_{10}[HV^{IV}{}_{16}V^{V}{}_2O_{42}(I)]\cdot 16H_2O$ (**5e**); $K_{10}[HV^{IV}{}_{16}V^{V}{}_2O_{42}(HCOO)]\cdot 15H_2O$ (**6**); $(NEt_4)_5[V^{IV}{}_{10}V^{V}{}_8O_{42}(I)]$ (**7**); $Na_6[H_7V^{IV}{}_{16}V^{V}{}_2O_{42}(VO_4)]\cdot 21H_2O$ (**8**).

The crystal structure analyses of the compounds show that the $\{V_{18}O_{42}\}$ shell can exist in two different structural types. The 24 μ_3 oxygen atoms form either the edges of a distorted rhombicuboctahedron (as in the case of the anion of **8**) or a so-called pseudorhombicuboctahedron, the "14th Archimedean body"[5] (as in the case of all other mentioned anions; Figure 1).[2,11,24,25] The latter polyhedron can be generated by a 45° rotation of one-half of the rhombicuboctahedron around one of its S_4 axes. The anion of **8** (Figure 2) has (idealized) T_d symmetry and can be regarded as an enlarged Keggin ion, in which all square planes ((100) and (110) type) of the rhombicuboctahedron spanned by the 24 innershell μ_3 oxygen atoms are capped by {VO} units (Figure 1).[15] In all other anions the idealized symmetry is D_{4d} (Figures 3−5).

Most of the differing structures of the cluster shells can be correlated with the type of encapsulated nucleophilic anions or molecules. In **8** the central, highly charged, tetrahedral $[VO_4]^{3-}$ unit interacts strongly with the V centers of the shell by forming covalent V−O−V bonds and "forces" the whole anion to adopt its inherent T_d symmetry (like in the classical Keggin anion; Figure 2). In contrast, the anions of the compounds **1a**−**7** represent a type of container, in which the attractive forces between the cluster shell and the anions with low charge densities or the neutral guests are only weak (Figures 3−5). In those structures 18 $\{VO_5\}$ square pyramids are linked to form a carcerand whereas in **8** also $\{VO_6\}$ octahedra occur according to the incorporation of oxygen atoms of the central unit into the coordination sphere of the V atoms of the shell.

(21) Nicolet XRD Corp., SHELXTL, Revision 4, 1983.
(22) *International Tables for Crystallography*; Kluwer Academic Publishers: Dordrecht, The Netherlands, 1992; Vol. C.
(23) Müller, A.; Reuter, H; Dillinger, S. *Angew. Chem., Int. Ed. Engl.* **1995**, *34*, 2311.
(24) Müller, A.; Penk, M. *Chem. Unserer Zeit* **1990**, *24*, 258.
(25) Müller, A.; Penk, M.; Döring, J. *Inorg. Chem.* **1991**, *30*, 4935.

Table 1. Information on Data Collection, Intensity Measurements, and Refinement Parameters for **1a**−**8**

	compd		
	$Cs_{12}[V^{IV}_{18}O_{42}(H_2O)]\cdot 14H_2O$ (**1a**)	$K_{12}[V^{IV}_{18}O_{42}(H_2O)]\cdot 16H_2O$ (**1b**)	$Rb_{12}[V^{IV}_{18}O_{42}(H_2O)]\cdot 19H_2O$ (**1c**)
empirical formula	$H_{30}Cs_{12}O_{57}V_{18}$	$H_{34}K_{12}O_{59}V_{18}$	$H_{40}O_{62}Rb_{12}V_{18}$
cryst dimens (mm)	0.3 × 0.25 × 0.1	0.3 × 0.3 × 0.25	0.2 × 0.2 × 0.15
space group	*Pbcn*	$P2_1/n$	$P\bar{1}$
a (pm)	1701.0(4)	1263.2(2)	1324.5(6)
b (pm)	1752.4(3)	3898.4(6)	1472.3(7)
c (pm)	2267.1(5)	1275.0(1)	1694.2(8)
α (deg)			83.66(4)
β (deg)		97.46(1)	89.72(4)
γ (deg)			82.99(4)
V (10^6 pm^3)	6758(2)	6225.5(15)	3259(3)
Z	4	4	2
d_{calc} (g cm^{-3})	3.40	2.52	3.03
μ(Mo Kα) (cm^{-1})	88.3	34.0	114.7
scan range (2*θ*) (deg)	4−45	4−48	3−45
scan width (*ω*) (deg)	1.6	1.6	1.2
scan speed (*ω*) (deg min^{-1})	6.0−29.3	6.0−29.3	3.9−29.3
T (K)	190	294	190
no. of measd reflcns	5097	10 836	7253
no. of unique obsd reflcns ($F > 4\sigma(F)$)	2835	6622	4103
no. of variables	267	574	516
$R = \sum\|\|F_o\| - \|F_c\|\|/\sum\|F_o\|$	0.093	0.062	0.079

	compd		
	$K_9[H_3V^{IV}_{18}O_{42}(H_2O)]\cdot 14H_2O\cdot 4N_2H_4$ (**1d**)	$K_{11}[H_2V^{IV}_{18}O_{42}(Cl)]\cdot 13H_2O\cdot 2N_2H_4$ (**2a**)	$K_9[H_4V^{IV}_{18}O_{42}(Br)]\cdot 14H_2O\cdot 4N_2H_4$ (**2b**)
empirical formula	$H_{49}K_9N_8O_{57}V_{18}$	$H_{36}ClK_{11}N_4O_{55}V_{18}$	$H_{48}BrK_9N_8O_{56}V_{18}$
cryst dimens (mm)	0.45 × 0.45 × 0.2	0.4 × 0.2 × 0.2	0.4 × 0.4 × 0.3
space group	*P*4/*ncc*	$P\bar{1}$	*P*4/*ncc*
a (pm)	1331.7(2)	1239.8(2)	1320.1(2)
b (pm)		1307.5(3)	
c (pm)	3643.5(10)	1868.2(4)	3649.1(7)
α (deg)		89.61(3)	
β (deg)		84.51(3)	
γ (deg)		74.13(3)	
V (10^6 pm^3)	6462(2)	2899(1)	6359(2)
Z	4	2	4
d_{calc} (g cm^{-3})	2.41	2.70	2.51
μ (Mo Kα) (cm^{-1})	31.6	37.1	38.4
scan range (2*θ*) (deg)	4−54	4−52	4−54
scan width (*ω*) (deg)	1.4	1.6	1.4
scan speed (*ω*) (deg min^{-1})	4.9−29.3	4.9−29.3	5.9−29.3
T (K)	203	193	198
no. of measd reflcns	7803	12 331	7932
no. of unique obsd reflcns ($F > 4\sigma(F)$)	2702	9343	2075
no. of variables	244	790	225
$R = \sum\|\|F_o\| - \|F_c\|\|/\sum\|F_o\|$	0.065	0.074	0.075

	compd		
	$K_9[H_4V^{IV}_{18}O_{42}(I)]\cdot 14H_2O\cdot 4N_2H_4$ (**2c**)	$K_{10}[H_3V^{IV}_{18}O_{42}(Br)]\cdot 13H_2O\cdot 0.5N_2H_4$ (**2d**)	$K_9[H_4V^{IV}_{18}O_{42}(NO_2)]\cdot 14H_2O\cdot 4N_2H_4$ (**3**)
empirical formula	$H_{48}IK_9N_8O_{56}V_{18}$	$H_{31}BrK_{10}N_8O_{55}V_{18}$	$H_{48}K_9N_9O_{58}V_{18}$
cryst dimens (mm)	0.5 × 0.4 × 0.3	0.45 × 0.4 × 0.35	0.25 × 0.2 × 0.05
space group	*P*4/*ncc*	$P\bar{1}$	*P*4/*ncc*
a (pm)	1317.9(3)	1246.4(5)	1320.6(5)
b (pm)		1310.4(6)	
c (pm)	3659.7(11)	1879.5(9)	3651.9(21)
α (deg)		89.47(4)	
β (deg)		83.85(3)	
γ (deg)		73.94(3)	
V (10^6 pm^3)	6356(3)	2932(2)	6368(5)
Z	4	2	4
d_{calc} (g cm^{-3})	2.56	2.62	2.47
μ(Mo Kα) (cm^{-3})	37.0	42.2	32.1
scan range (2*θ*) (deg)	4−57	4−54	4−50
scan width (*ω*) (deg)	1.3	1.3	1.6
scan speed (*ω*) (deg min^{-1})	4.9−29.3	4.9−29.3	5.9−29.3
T (K)	198	198	198
no. of measd reflcns	9234	13 467	6282
no. of unique obsd reflcns ($F > 4\sigma(F)$)	2958	10 347	1766
no. of variables	225	808	233
$R = \sum\|\|F_o\| - \|F_c\|\|/\sum\|F_o\|$)	0.065	0.062	0.089

Table 1 (Continued)

	compd		
	$Cs_{11}[H_2V^{IV}_{18}O_{42}(SH)]\cdot 12H_2O$ (**4**)	$K_{10}[HV^{IV}_{16}V^{V}_{2}O_{42}(Cl)]\cdot 16H_2O$ (**5a**)	$Cs_9[H_2V^{IV}_{16}V^{V}_{2}O_{42}(Br)]\cdot 12H_2O$ (**5b**)
empirical formula	$H_{27}Cs_{11}O_{54}SV_{18}$	$H_{33}ClK_{10}O_{58}V_{18}$	$H_{26}BrCs_9O_{54}V_{18}$
cryst dimens (mm)	0.15 × 0.15 × 0.1	0.45 × 0.3 × 0.05	0.25 × 0.15 × 0.1
space group	*Pbcn*	*P*$\bar{1}$	*C*2/*c*
a (pm)	1709.0(4)	1247.0(2)	2237.7(5)
b (pm)	1744.3(4)	1305.7(2)	1296.8(3)
c (pm)	2269.7(5)	1890.0(3)	2333.3(5)
α (deg)		88.39(1)	
β (deg)		83.50(1)	111.54(2)
γ (deg)		73.52(1)	
V (10^6 pm^3)	6766(3)	2932(2)	6298(3)
Z	4	2	4
d_{calc} (g cm^{-3})	3.24		3.25
μ(Mo Kα) (cm^{-1})	83.2		82.8
scan range (2*θ*) (deg)	4−50	4−50	4−50
scan width (*ω*) (deg)	1.6	1.6	1.6
scan speed (*ω*) (deg min^{-1})	3.9−29.3	3.9−29.3	3.9−29.3
T (K)	294	294	294
no. of measd reflcns	6810	11 192	12 339
no. of unique obsd reflcns ($F > 4\sigma(F)$)	3793	8100	3889
no. of variables	377	729	350
$R = \sum\|\|F_o\| - \|F_c\|\|\sum\|F_o\|$	0.072	0.071	0.083

	compd		
	$K_{10}[HV^{IV}_{16}V^{V}_{2}O_{42}(Br)]\cdot 16H_2O$ (**5c**)	$Cs_9[H_2V^{IV}_{16}V^{V}_{2}O_{42}(I)]\cdot 12H_2O$ (**5d**)	$K_{10}[HV^{IV}_{16}V^{V}_{2}O_{42}(I)]\cdot 16H_2O$ (**5e**)
empirical formula	$H_{33}BrK_{10}O_{58}V_{18}$	$H_{26}Cs_9IO_{54}V_{18}$	$H_{33}IK_{10}O_{58}V_{18}$
cryst dimens (mm)	0.3 × 0.25 × 0.2	0.2 × 0.1 × 0.1	0.8 × 0.3 × 0.05
space group	*P*$\bar{1}$	*C*2/*c*	*P*$\bar{1}$
a (pm)	1251.5(2)	2239.1(5)	1253.1 (4)
b (pm)	1307.0(2)	1296.0(2)	1307.4(4)
c (pm)	1887.2(8)	2335.2(5)	1890.7(8)
α (deg)	88.65(2)		88.23(3)
β (deg)	83.72(2)	111.41(1)	83.40(3)
γ (deg)	73.57(2)		73.42(3)
V (10^6 pm^3)	2943(3)	6308(2)	2948(4)
Z	2	4	2
d_{calc} (g cm^{-3})	2.65	3.30	2.70
μ(Mo Kα) (cm^{-1})	42.1	82.4	40.5
scan range (2*θ*) (deg)	4−50	4−50	4−54
scan width (*ω*) (deg)	1.3	1.6	1.8
scan speed (*ω*) (deg min^{-1})	3.9−29.3	3.9−29.3	3.9−29.3
T (K)	294	294	294
no. of measd reflcns	10 250	6184	13 874
no. of unique obsd reflcns ($F > 4\sigma(F)$)	7751	4073	10 752
no. of variables	723	358	733
$R = \sum\|\|F_o\| - \|F_c\|\|/\sum\|F_o\|$	0.073	0.056	0.063

	compd		
	$K_{10}[HV^{IV}_{16}V^{V}_{2}O_{42}(HCOO)]\cdot 15H_2O$ (**6**)	$(NEt_4)_5[V^{IV}_{10}V^{V}_{8}O_{42}(I)]$ (**7**)	$Na_6[H_7V^{IV}_{16}V^{V}_{2}O_{42}(VO_4)]\cdot 21H_2O$ (**8**)
empirical formula	$CH_{32}K_{10}O_{59}V_{18}$	$C_{40}H_{100}IN_5O_{42}V_{18}$	$H_{49}Na_6O_{67}V_{19}$
cryst dimens (mm)	0.8 × 0.2 × 0.025	0.25 × 0.2 × 0.15	
space group	*P*$\bar{1}$	*P*2$_1$/*n*	Cc[a]
a (pm)	1260.0(3)	1339.2 (9)	2048.8(9)
b (pm)	1306.0(3)	2303.6(6)	1507.3(7)
c (pm)	1872.8(4)	2636.0(5)	1893.6(8)
α (deg)	88.29(3)		
β (deg)	83.55(3)	90.28(4)	97.64(3)
γ (deg)	73.40(3)		
V (10^6 pm^3)	2935(2)	8132(6)	5796(4)
Z	2	4	4
d_{calc} (g cm^{-3})	2.60	1.93	2.55
μ(Mo Kα) (cm^{-1})	3.55	23.6	30.9
scan range (2*θ*) (deg)	4−52	3−50	4−52
scan width (*ω*) (deg)	1.3	1.2	1.2
scan speed (*ω*) (deg min^{-1})	4.9−29.3	3.9−29.3	7.3−29.3
T (K)	193	294	140
no. of measd reflcns	10 298	14 769	6320
no. of unique obsd reflcns ($F > 4\sigma(F)$)	6666	8058	4395
no. of variables	725	767	464
$R = \sum\|\|F_o\| - \|F_c\|\|/\sum\|F_o\|$	0.073	0.077	0.075

[a] Absolute structure parameter $\chi = 0.07(6)$ (Flack, H. D. *Acta Crystallogr.* **1983**, *A39*, 876).

Table 2. Atomic Coordinates ($\times 10^4$) and Isotropic Thermal Parameters $U(eq)^a$ ($pm^2 \times 10^{-1}$) for **1a**[b]

atom	*x*	*y*	*z*	*U*(eq)	atom	*x*	*y*	*z*	*U*(eq)
V(1)	1140(2)	4804(2)	1575(2)	11(1)	O(16)	−223(9)	3359(9)	890(7)	6(4)
V(2)	−867(2)	4243(2)	1088(2)	10(1)	O(17)	1526(10)	2451(9)	1586(8)	14(4)
V(3)	−448(2)	5415(2)	1943(2)	8(1)	O(18)	1269(9)	1998(9)	3186(8)	9(4)
V(4)	2077(3)	3383(2)	1710(2)	13(1)	O(19)	−1548(10)	3449(10)	1400(8)	19(4)
V(5)	769(2)	2834(2)	1007(2)	11(1)	O(20)	687(10)	1443(9)	2276(8)	10(4)
V(6)	−971(2)	2571(3)	1139(2)	12(1)	O(21)	−30(10)	2040(9)	3744(8)	11(4)
V(7)	2026(2)	3975(2)	2931(2)	10(1)	O(22)	0	3415(22)	2500	67(11)
V(8)	1654(3)	2015(2)	2382(2)	13(1)	Cs(1)	1113(1)	6997(1)	1943(1)	21(1)
V(9)	315(3)	1397(2)	3106(2)	12(1)	Cs(2)	−9(1)	6196(1)	402(1)	29(1)
O(1)	1619(10)	5411(10)	1201(8)	18(4)	Cs(3)	2576(1)	5856(1)	3741(1)	26(1)
O(2)	−1236(10)	4591(10)	466(9)	19(4)	Cs(4)	1395(1)	9916(1)	1947(1)	30(1)
O(3)	−664(10)	6299(9)	1711(8)	14(4)	Cs(5)	2820(1)	6626(1)	−415(1)	44(1)
O(4)	2953(10)	3395(9)	1401(8)	13(4)	Cs(6)	4979(2)	6039(2)	191(2)	121(2)
O(5)	1059(10)	2570(10)	366(9)	21(4)	O(23)	1201(18)	7573(18)	599(15)	87(10)
O(6)	−1431(10)	2204(10)	567(8)	19(4)	O(24A)	−1996(16)	5799(13)	−95(11)	40(6)
O(7)	2918(10)	4255(9)	3138(8)	14(4)	O(24B)	−2424(33)	5675(28)	−265(23)	37(19)
O(8)	2346(10)	1367(9)	2354(8)	17(4)	O(25)	3314(13)	7489(13)	−1512(11)	45(6)
O(9)	450(11)	519(10)	3385(9)	24(5)	O(26)	3526(22)	4843(21)	194(18)	25(9)
O(10)	−630(9)	5345(9)	2786(8)	8(4)	O(27A)	4261(28)	5931(26)	−1215(22)	22(12)
O(11)	1869(9)	4329(8)	2119(7)	5(4)	O(27B)	4466(32)	5972(29)	−1727(26)	89(17)
O(12)	35(10)	4844(9)	1318(8)	14(4)	O(28)	1963(13)	11100(12)	906(10)	37(6)
O(13)	1272(9)	3789(9)	1187(7)	8(4)	O(29)	135(29)	8215(26)	2734(21)	52(14)
O(14)	2152(10)	2981(9)	2508(8)	17(4)	O(30)	4823(51)	6833(48)	−875(40)	132(30)
O(15)	−1321(9)	4753(9)	1770(8)	9(4)	O(31)	6157(89)	4879(91)	530(72)	287(74)

[a] *U*(eq) is calculated as a third of the trace of the orthogonalized $\mathbf{U}_{ij}$ tensor. [b] Occupancy factors deviating from normal occupancy due to disorder: O(24A), 0.7; O(24B), 0.3; O(26), 0.5; O(27A), 0.4; O(27B), 0.6; O(29)−O(31), 0.5.

In the compounds **1a**−**7** the attractive and (the stronger) repulsive forces between the electrophilic (V^{n+}) and nucleophilic (O^{2-}) centers of the shell and the enclosed nucleophilic guests only approximately balance each other. According to basic MO calculations of Bénard and co-workers on an ab-initio level the electrostatic potential inside an overall negatively charged $\{V_{18}O_{42}\}$ cluster cage is negative.[26] However, the consideration of the crystal environment[27] leads to positive values of the potential thus supporting also our earlier assumption[23] that the cations of the crystal lattice have an important influence on the stabilization of the polyoxovanadate host−guest system. In this context it is worth noting that the spherical $\{V_{18}O_{42}\}$ shell with D_{4d} symmetry is preferentially formed in the case of relatively small and/or only slightly charged anions (monoanions like the halide anions) or *small* neutral molecules, respectively.

For the determination of the electronic structure and the number of V^{IV} centers of the described cluster compounds the following methods and/or data have been used (see also Table 5): (a) elemental analyses; (b) redox titrations; (c) $(V{=}O)_{term}$ values (obtained from IR spectra); (d) bond valence sums;[28] (e) average distances between the V atoms of the $\{V_{18}\ O_{42}\}$ shell and its center; (f) average V−V distances; (g) magnetic susceptibilities; (h) EPR spectra.

Analytical data, although very important, are not sufficient to determine unambiguously the precise number of V^{IV} centers of the V_{18} shells. Due to the relatively high molar masses of the studied compounds (∼2200−3500 g mol^{-1}) and the complex redox behavior of certain oxidizable components of some compounds (apart from V^{IV} centers, halide ions, hydrazine, nitrite, etc.) redox titrations are not necessarily accurate enough to distinguish between different systems with similar electron populations, e.g. between $\{V^{IV}{}_{18}O_{42}\}$ and $\{V^{IV}{}_{17}V^{V}O_{42}\}$ shells. Even a knowledge of the number of cations (and therefore the charge on the cluster anions) is—due to possible protonations of the cluster anions—not sufficient to determine the number of V^{IV} centers. As the hydrogen atoms themselves are in general not localized, their number and position cannot be obtained simply from difference Fourier maps.

Nevertheless, on the basis of analytical data in connection with the above-mentioned methods and/or data, it is now possible to distinguish between three basic types of cluster anions (see Table 5):

(**I**) The $V^{IV}{}_{18}O_{42}$ type with actual values of the average bond valence sums for V between 4.07 and 4.23, with rather low values of $(V{=}O)_{term}$ (ca. 950 cm^{-1}) and $\chi_M T$ values (260 K) between 3.4 and 2.7 emu K mol^{-1}.

(**II**) The $V^{IV}{}_{16}V^{V}{}_{2}O_{42}$ type with nonlocalized V^{IV} centers and actual values of the average bond valence sums between ca. 4.24 and 4.37, of $(V{=}O)_{term}$ between ca. 965 and 970 cm^{-1}, and of $\chi_M T$ (260 K) between ca. 1.9 and 2.4 emu K mol^{-1}.

(**III**) The $V^{IV}{}_{10}V^{V}{}_{8}O_{42}$ type with nonlocalized V^{IV} centers and correspondingly rather large average bond valence sums, high $(V{=}O)_{term}$ values and low $\chi_M T$ values (see Table 5 in the case of **7**).

For cluster cages with the same enclosed guest species, the average radius of the $\{V_{18}O_{42}\}$ shell and the average V−V distance are further useful criteria for distinguishing between the different types (Table 5).

Class **I** comprises "fully reduced" anions (18 V^{IV} centers) with neutral or anionic guests. The structures of the cluster anions are almost identical; slight differences concerning bond lengths and therefore the volume of the cluster shell can principally be attributed to the different kinds of encapsulated guests.

Compounds **1a**−**c** are synthesized under anaerobic conditions at high pH values (∼14) from aqueous vanadate solutions (Figure 3). Under these conditions only H_2O molecules are enclosed in the cluster shells—even if halide ions or other anionic species are present in the reaction medium. The existence of the "fully reduced" state can be unambiguously proven by manganometric redox titrations due to the presence of the redox inert H_2O guests. Further relevant characteristic properties include the low bond valence sums and low $\nu(V{=}O)$ values as

(26) Rohmer, M. M.; Devémy, J.; Wiest, R.; Bénard, M. *J. Am. Chem. Soc.* **1996**, *118*, 13007.
(27) Blaudeau, J. P.; Rohmer, M. M.; Bénard, M. *Bull. Soc. Chim. Fr.*, submitted for publication.
(28) Brown, I. D. In *Structure and Bonding in Crystals;* O'Keeffe, M., Navrotsky, A., Eds; Academic Press: New York, 1981; Vol. II, p 1.

Table 3. Atomic Coordinates ($\times 10^4$) and Isotropic Thermal Parameters $U(eq)^a$ ($pm^2 \times 10^{-1}$) for **6**[b]

atom	*x*	*y*	*z*	*U*(eq)	atom	*x*	*y*	*z*	*U*(eq)
V(1)	5349(1)	665(2)	2245(1)	17(1)	O(28)	1174(5)	3601(5)	964(4)	16(2)
V(2)	3920(1)	−92(1)	1351(1)	15(1)	O(29)	1688(6)	4939(6)	1945(4)	18(2)
V(3)	4546(1)	2510(1)	1251(1)	15(1)	O(30)	1903(6)	4793(6)	3246(4)	19(2)
V(4)	4847(1)	2344(1)	3206(1)	15(1)	O(31)	1717(6)	3308(5)	4310(3)	14(1)
V(5)	4211(1)	−214(1)	3308(1)	14(1)	O(32)	1274(6)	1542(5)	4418(4)	17(2)
V(6)	1469(2)	401(1)	1216(1)	18(1)	O(33)	778(6)	266(5)	3425(4)	18(2)
V(7)	2049(1)	2242(1)	530(1)	17(1)	O(34)	−1452(6)	938(6)	3054(4)	23(2)
V(8)	2400(1)	4182(1)	1061(1)	15(1)	O(35)	−1056(6)	3727(6)	984(4)	26(2)
V(9)	3027(1)	4762(1)	2436(1)	16(1)	O(36)	−133(6)	6187(6)	2905(4)	27(2)
V(10)	2853(2)	3936(1)	3922(1)	17(1)	O(37)	−505(7)	3460(7)	4919(4)	33(2)
V(11)	2668(1)	1916(1)	4533(1)	15(1)	O(38)	−696(6)	2436(6)	2191(4)	22(2)
V(12)	1874(1)	170(1)	4044(1)	15(1)	O(39)	−208(6)	4277(6)	2176(4)	20(2)
V(13)	1714(1)	−614(1)	2630(1)	16(1)	O(40)	−41(6)	4134(6)	3494(4)	20(2)
V(14)	−68(1)	3205(1)	1469(1)	16(1)	O(41)	−460(5)	2388(6)	3577(4)	18(2)
V(15)	592(1)	4945(1)	2764(1)	17(1)	O(42)	−2198(6)	4131(7)	3099(5)	37(2)
V(16)	332(1)	3004(1)	4202(1)	16(1)	C(1)	2272(9)	2149(9)	2541(6)	22(2)
V(17)	−315(1)	1287(1)	2878(1)	17(1)	O(100)	1398(10)	2090(14)	2408(8)	103(6)
V(18)	−900(1)	3540(2)	2913(1)	21(1)	O(101)	2905(10)	1682(11)	2941(7)	77(4)
O(1)	6660(6)	77(6)	2056(4)	28(2)	K(1)	7281(6)	2300(7)	1909(5)	76(5)
O(2)	4520(6)	−363(6)	2285(4)	20(2)	OK1	7281(6)	2300(7)	1909(5)	76(5)
O(3)	4687(5)	987(6)	1350(4)	18(2)	K(2)	2705(3)	6728(3)	−282(3)	79(2)
O(4)	5107(6)	2198(6)	2192(4)	19(2)	K(3)	880(4)	7081(3)	1551(2)	68(1)
O(5)	5009(5)	837(5)	3275(4)	16(2)	K(4)	5759(3)	−3070(2)	650(2)	53(1)
O(6)	4664(7)	−988(7)	772(4)	30(2)	K(5)	1349(2)	6893(2)	3752(1)	29(1)
O(7)	5586(6)	2556(6)	662(4)	23(2)	K(6)	−2409(2)	2176(2)	4356(2)	31(1)
O(8)	5993(6)	2463(6)	3436(4)	23(2)	K(7)	7407(3)	−570(3)	3491(2)	45(1)
O(9)	5091(6)	−1245(6)	3599(4)	22(2)	K(8)	1393(3)	4246(3)	5658(2)	56(1)
O(10)	2629(6)	−537(6)	1759(4)	18(2)	K(9)	6641(2)	163(3)	477(2)	45(1)
O(11)	2762(5)	832(5)	835(4)	16(2)	K(10)	4676(3)	2898(3)	5382(2)	51(1)
O(12)	3267(5)	2766(5)	733(4)	17(2)	K(11)	0	5000	0	78(2)
O(13)	3729(5)	3960(6)	1569(4)	18(2)	O(43)	−492(6)	8755(6)	4054(4)	27(2)
O(14)	3952(6)	3801(5)	3081(4)	16(2)	O(44)	416(7)	8081(7)	200(4)	31(2)
O(15)	3831(6)	2507(6)	4075(4)	17(2)	O(45)	−3898(7)	895(7)	4651(5)	36(2)
O(16)	3274(5)	454(5)	4177(4)	15(1)	O(46)	3012(12)	3721(12)	6469(8)	94(4)
O(17)	2838(5)	−656(5)	3263(4)	15(2)	O(47)	3411(9)	7204(9)	3874(6)	61(3)
O(18)	1496(6)	−1775(6)	2650(4)	23(2)	O(48)	−3945(7)	4021(8)	4700(5)	42(2)
O(19)	1178(7)	−303(6)	609(5)	33(2)	O(49)	5255(12)	5155(12)	3475(8)	91(4)
O(20)	2063(6)	2235(7)	−346(4)	27(2)	O(50)	−706(11)	6201(11)	1183(8)	86(4)
O(21)	2389(7)	5035(7)	421(4)	29(2)	O(51)	−799(12)	8991(12)	1808(8)	98(5)
O(22)	3326(7)	5891(6)	2415(4)	28(2)	O(52)	5050(13)	−4880(14)	653(9)	114(5)
O(23)	3003(6)	4718(6)	4540(4)	25(2)	O(53)	8300(19)	859(19)	972(13)	168(8)
O(24)	2815(6)	1920(6)	5376(4)	22(2)	O(54)	6618(38)	−5745(39)	1548(27)	182(18)
O(25)	1649(6)	−645(6)	4656(4)	23(2)	O(55)	3073(8)	7344(8)	1261(5)	44(2)
O(26)	570(6)	333(6)	2103(4)	20(2)	O(56)	7931(21)	−2240(21)	2603(15)	209(11)
O(27)	721(5)	1871(6)	994(4)	20(2)	O(57)	6235(20)	−2420(20)	2002(14)	188(9)

[a] *U*(eq) is calculated as a third of the trace of the orthogonalized $\mathbf{U}_{ij}$ tensor. [b] Occupancy factors deviating from normal occupancy due to disorder: K(1), OK(1), K(11), O(54), 0.5.

well as characteristic rather large high-temperature magnetic susceptibilities (see below as well as Table 5 and Figure 6). The encapsulation of H_2O molecules is supported by the fact that the positions of 12 alkali metal cations could be obtained from difference Fourier maps and that a protonation of the cluster shell is impossible due to the experimental conditions (pH 14). In fact, the absence of protons on the cluster shell and the resulting high negative charge can be considered to be the reason for the encapsulation of a *neutral* instead of *negatively charged* species. The average radius $r_{av}(V_{18})$ of the $\{V_{18}O_{42}\}$ shells (corresponding to the average $V-O(H_2O)$ distance) in the present case is 380.1 pm and the average V−V distance 295.9 pm. These values are slightly larger than the corresponding values of the other "fully reduced" compounds **2a**−**4** with encapsulated *anions* ($r_{av}(V_{18}) = 377.1$ pm; $d_{av}(V-V) = 293.6$ pm). This can *principally* be attributed to the fact that the electrostatic attraction between *negatively* charged guests and the V^{IV} centers is *relatively* stronger.

The incorporation of *anions* in a "fully reduced" shell succeeds when the experimental parameters of the synthetic route leading to **1a**−**c** are suitably changed. The compounds **2a**−**3** can be obtained under strongly reducing conditions at lower pH values (∼10; allowing protonation of the shell) by addition of the corresponding anionic species to a reaction medium that contains the "fully reduced" compound $K_{12}[V^{IV}_{18}O_{42}(H_2O)]\cdot 16H_2O$ (**1b**) as educt. **4** is synthesized under inert atmospheric conditions at pH 8 by passing H_2S into a reduced aqueous vanadate solution.

The IR spectra of **1d**−**2d** show two bands at ∼1530 and 1115 cm^{-1} which are not observed in the spectra of the other compounds. They have to be assigned to the $\delta(NH_2)$ and $\rho_r(NH_2)$ vibrations of the lattice N_2H_4 molecules. Their presence is further supported by N analyses and redox titrations. However, due to disorder problems the positions could not be determined unambiguously from difference Fourier maps. The same holds for the hydrogen atom positions of the encapsulated species and on the shells in **1a**−**d**, **4**, and **6**. This means that from X-ray data alone it is for instance not possible to distinguish in the case of **4** between the possible guests H_2S, HS^-, or even S^{2-}. The presence of S^{2-} can be regarded as practically impossible because of the pH value of the reaction medium (pH ∼ 8) and because of the high nucleophilicity/basicity of the dianion, which does not allow weak host−guest interactions, a prerequisite for the formation of the cage system.

Table 4. Atomic Coordinates ($\times 10^4$) and Isotropic Thermal Parameters $U(eq)^a$ ($pm^2 \times 10^{-1}$) for **7**[b]

atom	*x*	*y*	*z*	*U*(eq)	atom	*x*	*y*	*z*	*U*(eq)
V(1)	5956(2)	7674(1)	−590(1)	35(1)	O(37)	9722(6)	6761(3)	500(3)	36(2)
V(2)	5514(2)	8553(1)	137(1)	34(1)	O(38)	10050(6)	7838(4)	471(3)	36(2)
V(3)	5014(2)	7002(1)	180(1)	36(1)	O(39)	7943(6)	8127(3)	1940(3)	33(2)
V(4)	7325(2)	6745(1)	−518(1)	33(1)	O(40)	7581(7)	7033(4)	1964(3)	40(2)
V(5)	7818(2)	8299(1)	−556(1)	32(1)	O(41)	9225(6)	6858(4)	1491(3)	37(2)
V(6)	7859(2)	9179(1)	597(1)	36(1)	O(42)	9558(6)	7911(3)	1479(3)	33(2)
V(7)	6142(2)	8901(1)	1183(1)	35(1)	N(1)	7576(9)	1394(5)	1361(4)	49(3)
V(8)	4987(2)	7859(1)	1337(1)	37(1)	C(1)	7110(25)	2005(15)	1286(12)	163(12)
V(9)	5421(2)	6631(1)	1251(1)	36(1)	C(2)	7091(18)	2167(10)	715(9)	105(7)
V(10)	6845(2)	5979(1)	662(1)	37(1)	C(3)	8502(27)	1288(15)	1078(12)	168(12)
V(11)	8779(2)	6249(1)	236(1)	36(1)	C(4)	9329(19)	1772(11)	1314(9)	110(8)
V(12)	9733(2)	7304(1)	−73(1)	34(1)	C(5)	7748(19)	1394(10)	1936(9)	109(7)
V(13)	9473(2)	8498(1)	168(1)	34(1)	C(6)	8230(32)	657(18)	1989(15)	219(17)
V(14)	8747(2)	8604(1)	1498(1)	35(1)	C(7)	6943(28)	877(16)	1218(13)	181(14)
V(15)	6743(2)	7689(1)	2025(1)	33(1)	C(8)	5804(17)	1003(9)	1420(8)	94(6)
V(16)	8042(2)	6393(1)	1558(1)	36(1)	N(2)	7773(9)	4609(5)	−898(4)	44(3)
V(17)	10021(2)	7309(1)	1035(1)	35(1)	C(9)	7125(11)	5014(6)	−586(5)	53(4)
V(18)	8787(2)	7457(1)	1947(1)	38(1)	C(10)	6040(13)	4825(8)	−550(6)	75(5)
I(1)	7398(1)	7573(1)	673(1)	33(1)	C(11)	7349(12)	4548(7)	−1450(5)	58(4)
O(1)	5350(7)	7712(4)	−1112(3)	48(2)	C(12)	7325(15)	5128(8)	−1731(7)	90(6)
O(2)	4698(7)	8975(4)	−86(3)	44(2)	C(13)	7773(14)	3999(8)	−677(6)	74(5)
O(3)	3998(7)	6754(4)	−28(3)	50(2)	C(14)	8077(16)	3949(9)	−151(7)	94(6)
O(4)	7305(7)	6387(4)	−1030(3)	42(2)	C(15)	8842(12)	4871(7)	−891(6)	59(4)
O(5)	8012(7)	8613(3)	−1081(3)	38(2)	C(16)	9555(13)	4552(8)	−1239(6)	72(5)
O(6)	8068(7)	9851(4)	552(3)	50(2)	N(3)	7064(13)	4210(5)	1750(4)	72(5)
O(7)	5589(7)	9461(4)	1402(4)	54(3)	C(17)	7763(16)	4257(9)	1336(7)	88(6)
O(8)	3977(8)	8004(4)	1626(3)	57(3)	C(18)	8424(21)	3739(12)	1285(10)	151(11)
O(9)	4592(7)	6229(4)	1487(3)	47(2)	C(19)	7599(14)	4124(8)	2274(6)	73(5)
O(10)	6609(7)	5307(3)	638(3)	46(2)	C(20)	8496(16)	4529(10)	2355(8)	106(7)
O(11)	9360(7)	5699(4)	58(4)	52(2)	C(21)	6471(12)	4763(7)	1741(6)	62(4)
O(12)	10705(7)	7192(4)	−394(3)	51(2)	C(22)	5614(15)	4805(9)	2089(7)	88(6)
O(13)	10347(7)	8889(4)	−48(3)	45(2)	C(23)	6377(21)	3681(12)	1724(10)	136(10)
O(14)	9339(7)	9050(4)	1849(3)	45(2)	C(24)	5670(24)	3688(14)	1272(11)	183(14)
O(15)	6465(7)	7742(4)	2615(3)	46(2)	N(4)	2429(9)	7296(5)	2658(4)	52(3)
O(16)	8326(8)	5888(4)	1939(3)	51(2)	C(25)	3133(12)	6924(7)	2356(6)	59(4)
O(17)	11134(6)	7187(4)	1194(3)	42(2)	C(26)	3653(13)	6436(7)	2620(6)	71(5)
O(18)	9339(7)	7402(4)	2480(3)	52(3)	C(27)	2931(12)	7552(7)	3112(6)	61(4)
O(19)	6466(6)	8427(3)	−390(3)	30(2)	C(28)	3783(14)	7980(8)	2992(7)	84(6)
O(20)	5083(7)	7795(4)	−22(3)	39(2)	C(29)	2006(12)	7751(6)	2307(5)	57(4)
O(21)	5970(6)	6888(3)	−343(3)	36(2)	C(30)	1351(12)	8182(7)	2579(6)	64(4)
O(22)	7360(6)	7534(3)	−708(3)	33(2)	C(31)	1582(11)	6880(6)	2870(5)	54(4)
O(23)	8211(6)	8855(3)	−44(3)	36(2)	C(32)	1116(13)	6491(8)	2480(6)	72(5)
O(24)	6485(6)	9038(3)	490(3)	34(2)	N(5)	2341(10)	9552(5)	1042(5)	56(3)
O(25)	5139(6)	8440(4)	833(3)	38(2)	C(33A)	3361(21)	9534(12)	794(10)	43(6)
O(26)	4787(7)	7248(4)	873(3)	39(2)	C(33B)	2639(52)	9774(29)	555(24)	160(24)
O(27)	5614(7)	6367(4)	556(3)	39(2)	C(34)	3839(16)	10088(9)	623(7)	86(6)
O(28)	7390(7)	6181(3)	22(3)	37(2)	C(35A)	1633(21)	9869(12)	687(10)	44(6)
O(29)	8727(6)	6787(3)	−320(3)	34(2)	C(35B)	1378(94)	9787(51)	1213(43)	309(56)
O(30)	9086(6)	7958(3)	−350(3)	36(2)	C(36)	597(18)	10017(10)	947(8)	96(6)
O(31)	9095(6)	8794(3)	813(3)	34(2)	C(37A)	1849(47)	8821(26)	1135(21)	131(19)
O(32)	7512(7)	9005(4)	1285(3)	40(2)	C(37B)	2566(37)	8969(20)	1163(17)	96(13)
O(33)	6027(6)	8309(4)	1669(3)	37(2)	C(38)	2304(18)	8495(11)	725(9)	110(8)
O(34)	5658(6)	7253(3)	1711(3)	32(2)	C(39)	2545(23)	9956(13)	1476(11)	137(10)
O(35)	6650(7)	6256(3)	1355(3)	39(2)	C(40)	3240(26)	9721(15)	1894(12)	167(12)
O(36)	8215(6)	6084(3)	870(3)	33(2)					

[a] *U*(eq) is calculated as a third of the trace of the orthogonalized $\mathbf{U}_{ij}$ tensor. [b] Occupancy factors deviating from normal occupancy due to disorder: C(33A/B), C(35A/B), C(37A/B), 0.5.

The presence of SH^- could principally but not necessarily be supported by chemical deliberations regarding its existence in aqueous solution under relevant conditions. The average radius of the $\{V_{18}O_{42}\}$ shell (376.3 pm) is comparable to the values obtained for other clusters containing anionic guests (mean value 377.1 pm; see corresponding arguments above). Nevertheless, the presence of H_2S as guest and a corresponding lower degree of protonation of the shell cannot be excluded.

In the anion of **3** a nitrite anion is encapsulated in a $\{V_{18}O_{42}\}$ shell. The nitrogen atom is approximately located in the center of the shell, but due to an existing disorder the positions of the oxygen atoms cannot be obtained from difference Fourier maps. However, the nature of the anion was unambiguously determined from IR data (ν_{as}(NO) 1228 cm^{-1}) and by the qualitative test for NO_2^- with α-naphthylamine and sulfanilic acid corresponding to the method of Lunge.[29]

Compounds of type **II** (see above) contain mixed-valence anions (type III according to the classification of Robin and Day[30]) with encapsulated anions. The corresponding syntheses are carried out in the presence of air at lower pH values (between 7 and 9) than those used for most of the compounds of type I. The anionic guest species seems to "prefer" a less reduced host system resulting in *relatively* weaker repulsive interactions between host and guest. The compounds of this class have

(29) Jander, G.; Blasius, E. *Handbook of Analytical and Preparative Inorganic Chemistry*, 13th ed.; Hirzel: Stuttgart, Germany, 1989; p 201.
(30) Robin, M. B.; Day, P. *Adv. Inorg. Chem. Radiochem.* **1967**, *10*, 247.

Table 5. Characteristic Physical Data for **1a**−**8** Belonging to the Three Different Compound Types **I**−**III** with Different Electron Populations

shell type	compd	bond valence sum	av bond valence sum	$r_{av}(V_{18})$ (pm)[a]	$d_{av}(V-V)$ (pm)[b]	$\nu(V{=}O)$ (cm^{-1})	$\chi_M T$ (260 K) (emu mol^{-1} K)
$V^{IV}{}_{18}O_{42}$	$Cs_{12}[V^{IV}{}_{18}O_{42}(H_2O)]\cdot 14H_2O$ (**1a**)	3.83−4.27	4.07	379.8	296.0	950	3.4
	$K_{12}[V^{IV}{}_{18}O_{42}(H_2O)]\cdot 16H_2O$ (**1b**)	4.01−4.32	4.12	380.3	296.1	950	3.1
	$Rb_{12}[V^{IV}{}_{18}O_{42}(H_2O)]\cdot 19H_2O$ (**1c**)	4.01−4.34	4.17	379.8	295.7	950	
	$K_9[H_3V^{IV}{}_{18}O_{42}(H_2O)]\cdot 14H_2O\cdot 4N_2H_4$ (**1d**)	4.06−4.10	4.08	380.4	295.9	952	
	$K_{11}[H_2V^{IV}{}_{18}O_{42}(Cl)]\cdot 13H_2O\cdot 2N_2H_4$ (**2a**)	4.08−4.42	4.19	376.8	293.6	954	3.1
	$K_9[H_4V^{IV}{}_{18}O_{42}(Br)]\cdot 14H_2O\cdot 4N_2H_4$ (**2b**)	4.14−4.38	4.23	376.4	292.9	953	2.9
	$K_9[H_4V^{IV}{}_{18}O_{42}(I)]\cdot 14H_2O\cdot 4N_2H_4$ (**2c**)	3.92−4.21	4.12	377.5	293.7	950	2.9
	$K_{10}[H_3V^{IV}{}_{18}O_{42}(Br)]\cdot 13H_2O\cdot 0.5N_2H_4$ (**2d**)	4.07−4.32	4.16	377.2	294.0	948	
	$K_9[H_4V^{IV}{}_{18}O_{42}(NO_2)]\cdot 14H_2O\cdot 4N_2H_4$ (**3**)	4.11−4.31	4.21	377.7	294.1	953	2.7
	$Cs_{11}[H_2V^{IV}{}_{18}O_{42}(SH)]\cdot 12H_2O$ (**4**)	4.10−4.37	4.19	376.3	293.2	950	2.8
$V^{IV}{}_{16}V^{V}{}_2O_{42}$	$K_{10}[HV^{IV}{}_{16}V^{V}{}_2O_{42}(Cl)]\cdot 16H_2O$ (**5a**)	4.17−4.53	4.32	375.2	292.8	965	2.4
	$Cs_9[H_2V^{IV}{}_{16}V^{V}{}_2O_{42}(Br)]\cdot 12H_2O$ (**5b**)	4.18−4.50	4.37	374.7	292.3	970	2.2
	$K_{10}[HV^{IV}{}_{16}V^{V}{}_2O_{42}(Br)]\cdot 16H_2O$ (**5c**)	4.10−4.44	4.25	375.7	293.1	965	2.2
	$Cs_9[H_2V^{IV}{}_{16}V^{V}{}_2O_{42}(I)]\cdot 12H_2O$ (**5d**)	4.12−4.43	4.29	375.3	292.8	970	
	$K_{10}[HV^{IV}{}_{16}V^{V}{}_2O_{42}(I)]\cdot 16H_2O$ (**5e**)	4.12−4.49	4.27	375.9	293.4	965	
	$K_{10}[HV^{IV}{}_{16}V^{V}{}_2O_{42}(HCOO)]\cdot 15H_2O$ (**6**)	4.08−4.65	4.24	376.4	293.8	968	2.2
	$Na_6[H_7V^{IV}{}_{16}V^{V}{}_2O_{42}(VO_4)]\cdot 21H_2O$ (**8**)	3.85−4.58	4.29	373.2	293.2	970	1.9
$V^{IV}{}_{10}V^{V}{}_8O_{42}$	$(NEt)_5[V^{IV}{}_{10}V^{V}{}_8O_{42}(I)]$ (**7**)	4.40−4.73	4.59	372.7	290.5	995	0.9

[a] Average distance between the V atoms of the $\{V_{18}O_{42}\}$ shell and its center. [b] Average V−V distance.

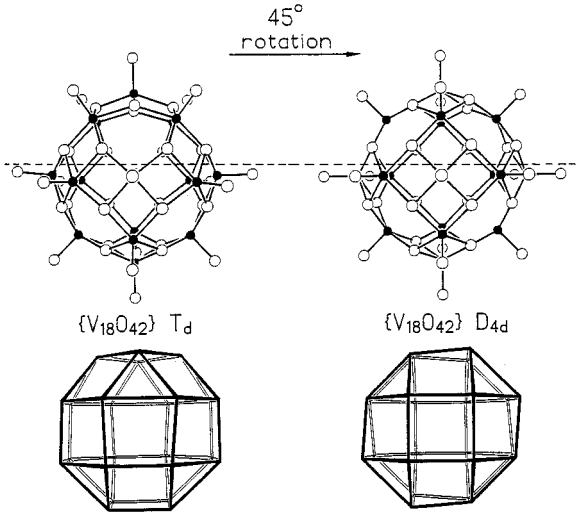

Figure 1. Depiction of the $\{V_{18}O_{42}\}$ cluster shells in $[H_7V_{18}O_{42}(VO_4)]^{6-}$ (left) and $[H_xV_{18}O_{42}(X)]^{y-}$ (X = H_2O, Cl^-, Br^-, I^-, SH^-, NO_2^-, $HCOO^-$; right). The V atoms are represented as black and the O atoms as white spheres, respectively. A rotation by 45° of one of the shell halves around one of its S_4 axes transforms the O_{24} rhombicuboctahedron of the bridging oxygen atoms of the anion $[H_7V_{18}O_{42}(VO_4)]^{6-}$ into the O_{24} pseudorhombicuboctahedron (the so-called "14th Archimedean body") of the bridging oxygen atoms in $[H_xV_{18}O_{42}(X)]^{y-}$.

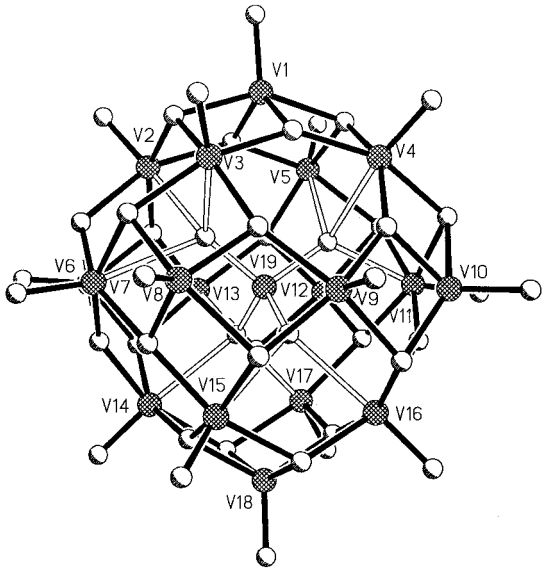

Figure 2. Ball-and-stick representation of the cluster anion of **8**.

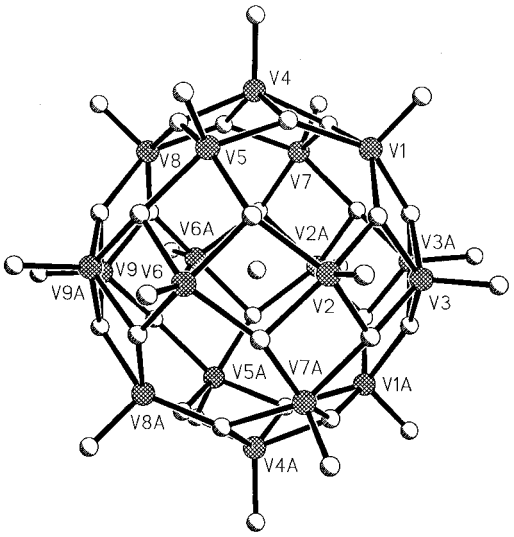

Figure 3. Ball-and-stick representation of the cluster anion of **1a**.

characteristic bond valence sums for V between ca. 4.24 and 4.37, $\nu(V{=}O)$ values between ca. 965 and 970 cm^{-1}, and high-temperature (260 K) $\chi_M T$ values between ca. 1.9 and 2.4 emu K mol^{-1}, as shown in Figure 6. The basic structure of the cluster shells is almost identical to those determined for **2a**−**4**.

In **6** a formate ion is encapsulated in the cluster shell (Figure 4). In contrast to **3**, the oxygen atoms in this case are not disordered—probably due to the relatively larger size of the guest. Anyhow, the distances to the vanadium centers of the shell are larger than 260 pm which means still too long for "normal" covalent bonds. The (anionic) nature of the enclosed guest is confirmed by nearly equal C−O distances (118 and 119 pm) and the positions of the corresponding $\nu_{as}(COO)$ (1595 cm^{-1}) and $\nu_s(COO)$ (1350 cm^{-1}) bands in the IR spectrum.

For class **III** there is so far only the compound **7** (see Figure 5) with a remarkably small number of V^{IV} centers which is apparent from the very low high-temperature $\chi_M T$ value (0.9 emu K mol^{-1} at 260 K), the rather high $\nu(V{=}O)$ frequency (995 cm^{-1}), and the comparatively high average V bond valence sum (4.59). The relatively small number of V^{IV} centers can be attributed to the fact that the cluster compound $(NH_4)_8[V^{IV}{}_{12}V^{V}{}_6O_{42}(SO_4)]\cdot 25H_2O$ was used as starting material for

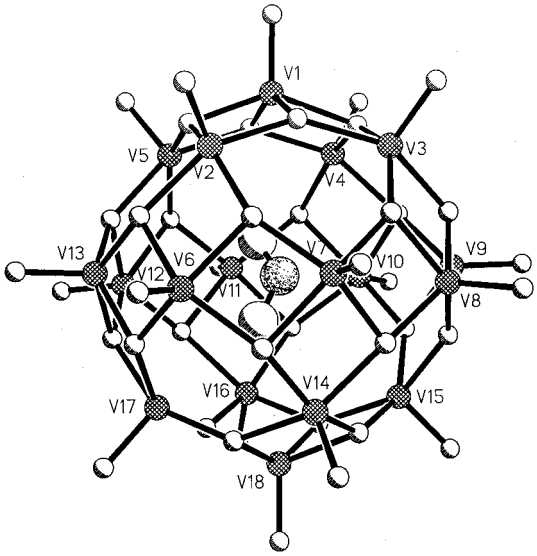

Figure 4. Ball-and-stick representation of the cluster anion of **6**.

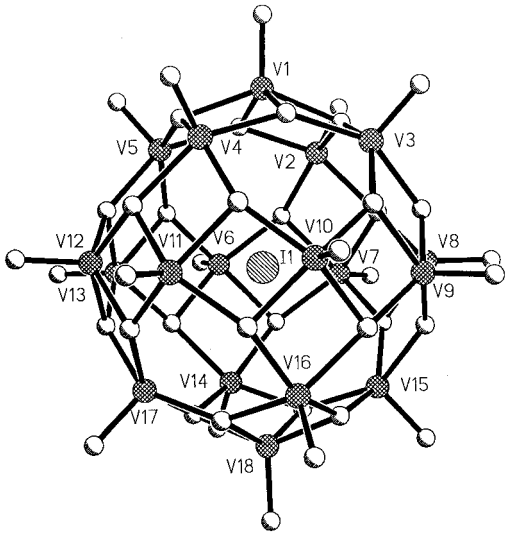

Figure 5. Ball-and-stick representation of the cluster anion of **7**.

the synthesis.[15] The number of V^{IV} centers was unambiguously determined from analytical data and the results of the single-crystal X-ray structure analysis. The mean bond valence sum for the oxygen atoms of the cluster is 1.97, indicating that no protonation takes place and the positions of five NEt_4^+ cations were found in difference Fourier maps. The small number of V^{IV} centers is also apparent from the average radius of the $\{V_{18}O_{42}\}$ shell and the average V−V distances (Table 5). These values are, as expected, smaller compared to those of the equivalent compounds **2c**, **5d**, and **5e** with encapsulated I^- ions as a smaller number of V^{IV} centers corresponds to a lower population of weakly antibonding levels.

Whereas in the container compounds **1a**−**7** the guest seems to "hover" inside the cavity (without being an integral component of the cluster shell) the situation in the case of **8** is different (Figure 2). In that case we have a covalently bonded $\{VO_4\}$ central unit with related short $V_{shell}-O_{centr.}$ bonds (∼239 pm). The $\{VO_4\}$ unit itself shows, as expected, approximately the same V−O distances (171 pm) as those in orthovanadates (172 pm).[31]

The classification of the compounds described within the scope of this article is justified by susceptibility and EPR measurements (Figure 6). Compound **1a**, if treated in oxygen-free atmosphere, shows the largest high-temperature magnetic susceptibility, $\chi_M T$ (260 K) = 3.4 emu K mol^{-1}. The $\chi_M T$ value decreases on lowering the temperature showing a marked decrease of the slope around 40 K and the tendency to go through a plateau (Figure 7). Below 15 K a much faster decrease of $\chi_M T$ is observed, with $\chi_M T$ approaching 0.4 at 2.8 K. A similar behavior is observed for **1b**. The high-temperature susceptibilities of **2a**−**4** containing anionic guests are slightly lower than that measured for **1a**, and the decrease of $\chi_M T$ on lowering the temperature is less pronounced. After contact with air for only a few hours, compound **1a** shows a different temperature dependence of $\chi_M T$ resembling that observed for the compounds of the second class ($V^{IV}_{16}V^{V}_{2}$; Figure 7). At high temperature (260 K) their $\chi_M T$ values are significantly smaller than those of class **I** ranging from ca. 2.4 emu K mol^{-1} for **5a** to ca. 1.9 emu K mol^{-1} for **8**. The fact that **8** has the lowest $\chi_M T$ value we attribute to the presence of the VO_4^{3-} anion in the center, which is not "hovering" but is covalently bound to the shell, thus providing additional pathways for transmitting the magnetic interactions. Comparison with the magnetic data of similar clusters[32] which encapsulate H_2O and Cl^- suggests that the magnetic measurements were carried out on partly oxidized compounds and, thus, are not in agreement with the formula. Furthermore, the interpretation of the magnetic data becomes flawed by the assumption that the spin state at a given temperature can be directly obtained from the χT value at that temperature. In Figure 6, $\chi_M T$ values observed for **7** are also given. The high-temperature (260 K) value of $\chi_M T$ is only 0.9 emu K mol^{-1} and decreases rapidly with decreasing temperature. At low temperature an almost constant $\chi_M T$ value of 0.05 emu K mol^{-1} is observed, which we attribute to a small impurity of V(IV).

A common feature of the whole series of compounds is the presence of strong antiferromagnetic coupling interactions. The $\chi_M T$ value expected for 18 V(IV) $S = {}^1/_2$ centers with $g = 1.97$ is in fact 6.53 emu K mol^{-1}. From analysis of the bond valence sums and charge considerations, the lowest average oxidation state is observed for compounds **1a**−**4**. This is also in agreement with the fact that by exposing **1a** to atmospheric dioxygen the magnetic behavior changes, resembling that of compounds **5a**−**6** and **8** for which (as mentioned above) analytical and spectroscopical data and the information obtained from single-crystal structure analysis suggest the presence of 16 ± 1 V(IV) and 2 ± 1 V(V) centers (Figure 7). In agreement with the formula obtained from all data for **7** a completely different magnetic behavior is observed.

Comparison of the structural parameters of the V coordination spheres suggests that in the mixed-valence systems **5a**−**8** the electronic charge is fully delocalized. Quantitative analysis of the magnetic data therefore cannot be carried out for compounds **5a**−**8**. In the case of the totally reduced species **1a**,**b**, the calculation of the energy of the 48 620 spin levels arising from the coupling of the 18 $S = {}^1/_2$ centers has been performed by exploiting the symmetry of the total spin using a method based on *irreducible tensor operators*[33] (with the Hamiltonian operator given as $\hat{H} = \sum_{i<j} J_{ij}\hat{S}_i\hat{S}_j$). The Hamiltonian matrix is calculated for the different S values, ranging from 0 to 9. The calculation has been simplified by taking into account the idealized D_{4d} symmetry of the cluster. Nevertheless, the dimensions of the matrices that have to be diagonalized reach 3382 × 3382 for $S = 2$. Therefore, they have not allowed a true fitting procedure

(31) Wells, A. F. *Structural Inorganic Chemistry*, 5th ed.; Clarendon Press: Oxford, U.K., 1984; p 567.

(32) Yamase, T.; Ohtaka, K.; Suzuki, M. *J. Chem. Soc., Dalton Trans.* **1996**, 283.

(33) Gatteschi, D.; Pardi, L. *Gazz. Chim. Ital.* **1993**, *123*, 231.

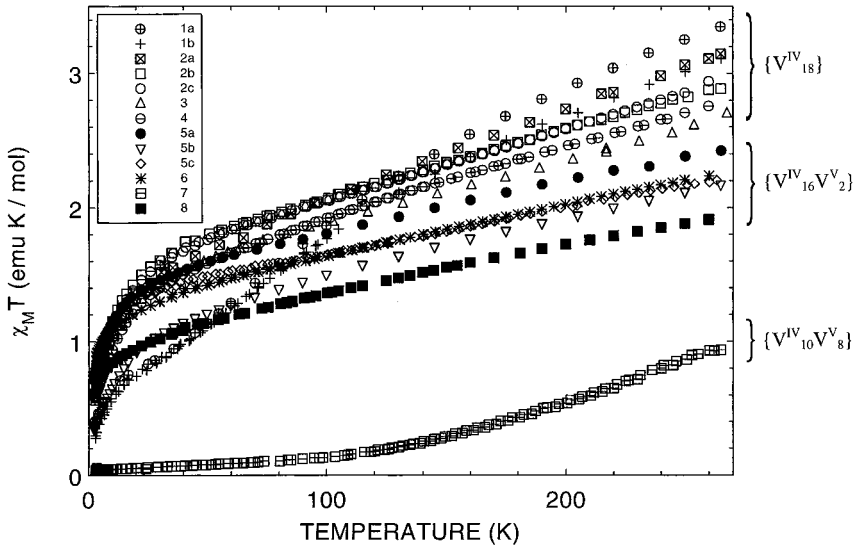

Figure 6. Temperature dependence of χT for **1a**−**8**.

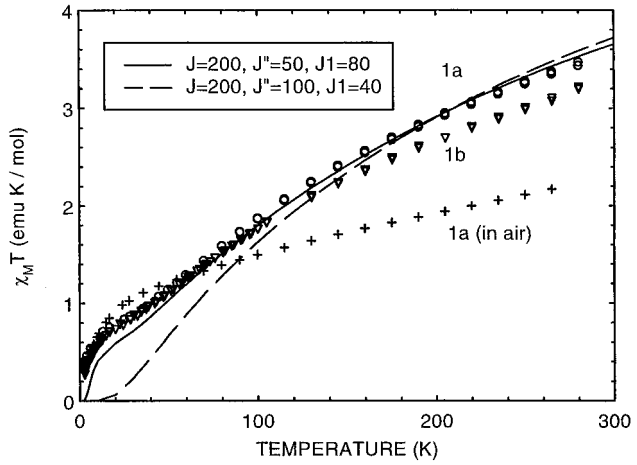

Figure 7. Temperature dependence of χT (measured and calculated) for **1a** and **1b**. The fitting has been done as described in the text.

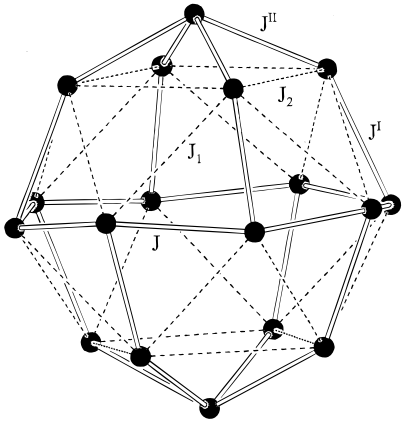

Figure 8. Spin topology of the cluster anion of **1a**.

and only a limited set of parameters for the magnetic interactions relating to the different bridges has been tested. Some of these results are reported in Figure 7.

The spin topology of the "fully reduced" compound **1a** containing 18 $S = {}^1/_2$ centers is depicted in Figure 8. Of the 48 connections between the 18 paramagnetic centers, 24 involve single μ_3-oxo bridges (dashed lines in the scheme) with a V−V average distance of 379.8 pm and the other 24 involve double μ_3-oxo bridges (solid lines) with an average V−V distance of 296 pm. In the idealized D_{4d} symmetry only five different coupling constants are present, as shown in Figure 8.

If we consider that the interactions through the double μ_3-oxo bridges are antiferromagnetic and dominate over the others ($J1$, $J2 << J$, J^{I}, J^{II}), the spin structure of the ground state is characterized by $S = 0$ and by a regular decrease of $\chi_{\mathrm{M}}T$ on reducing the temperature. The quasi-plateau in $\chi_{\mathrm{M}}T$ observed for **1a**,**b** could have originated through the presence of states with $S > 0$, probably $S = 1$ or 2, close to the diamagnetic ground state.

The spin topology of the cluster is such that the interactions mediated by the single μ_3-oxo bridges are in conflict with the previous ones and are also arranged in triangles. If they are not too weak, they can be the origin of the observed magnetic behavior.

We have assumed that J, J^{I} are equal and antiferromagnetic ($J = J^{\mathrm{I}} = 200$ cm^{-1}), stronger than J^{II} (100 cm^{-1}), and much stronger than $J1$ and $J2$ (40 cm^{-1}). The calculated $\chi_{\mathrm{M}}T$ is almost zero below 20 K, and the agreement with the experimental data is very poor.

In order to obtain a reasonable agreement $J1$ and $J2$ must be increased to overcome at least one interaction mediated by the double μ_3-oxo bridges (as shown in Figure 7), where the curve was calculated with $J = J^{\mathrm{I}} = 200$ cm^{-1}, $J^{\mathrm{II}} = 50$ cm^{-1}, and $J1 = J2 = 80$ cm^{-1}. Due to the large number of parameters and at least five exchange constants assuming the highest possible symmetry of the cluster, other sets of parameters could give similar results. However, our hypothesis that the observed behavior can be due to the presence of conflicting interactions through the single μ_3-oxo bridges seems to be correct.

It is surprising that magnetic interactions involving V−V distances of ca. 370 pm are comparable in strength with those characterized by a much shorter distance (ca. 300 pm); however, a systematic investigation of parameters and calculations on several samples is necessary in order to discuss further this point. Moreover, we see in Figure 6 that the low-temperature magnetic behavior changes within the compounds of class **I** on changing the guest inside the cavity. The guest seems to influence the magnetic interactions, and therefore, it can affect significantly the values of the coupling constants we have estimated.

The magnetic behavior of this class of clusters has been found to be very sensitive to the oxidation states and therefore to the number of electronic holes delocalized on the 18 sites. In fact, the average high temperature χT values per V^{IV} center reduces from 0.17 for the "fully reduced" $\{V^{IV}{}_{18}\}$ compounds to 0.14

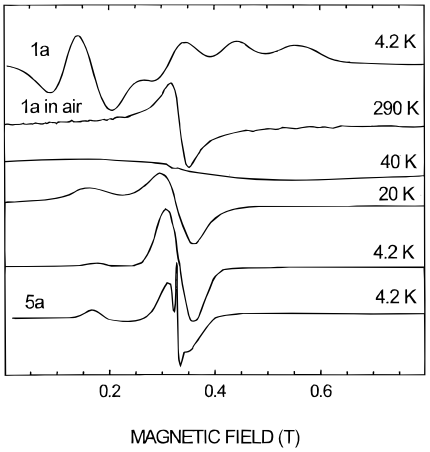

Figure 9. EPR spectra of solid samples of **1a** and **5a**.

for the $\{V^{IV}_{16}V^{V}_{2}\}$ type and to 0.09 emu K mol^{-1} for $\{V^{IV}_{10}V^{V}_{8}\}$. It is interesting to note that when 10 3d electrons are present in the cluster, as in **7**, the compound becomes practically diamagnetic at 100 K. We can justify this behavior with a lower degree of competition between antiferromagnetic interactions (which is called also spin frustration) due to the reduced number of paramagnetic centers. Furthermore, it is a well-established fact that electron delocalization can favor spin pairing.

Precious information on the oxidation state of the cluster is also provided by EPR spectra recorded on polycrystalline samples. In Figure 9 the spectrum recorded on **1a** at liquid-helium temperature is shown. Even if a detailed analysis is not the aim of this article, we can suggest that the observed spectrum is that of a spin state with $S > 1$ affected by a sizable zero field splitting, which is still populated at low temperature, in agreement with our interpretation of the magnetic data of the "fully reduced" clusters.

By exposure of **1a**,**b** to atmospheric oxygen, the EPR spectra change dramatically as shown in Figure 9 where the EPR spectra recorded on **1a** at four different temperatures are reported.[34] A single line is observed at room temperature with $\Delta H_{pp} = 320$ G and $g = 1.99$. Below 100 K the line width increases on decreasing the temperature and the line becomes very pronounced around 40 K with $\Delta H_{pp} = 4000$ G. Below 35 K the line narrows again showing an intense feature around 1600 G. At 4.2 K the principal line has ΔHpp = 500 G and $g = 1.98$ and the low-field absorption is still present even if much less intense than in the principal one. It is interesting to note that the EPR spectra of compounds **5a**,**c**,**e** resemble those of **1a** kept in contact with air, as shown in Figure 9 where the EPR spectrum of **5a** at 4.2 K is reported. The temperature dependence of the line width is also very similar, but a strong, narrow signal with $g_{\perp} = 1.924$ and $g_{II} = 1.989$, which we attribute to a V(IV) impurity, dominates above 50 K. We attribute the anomaly observed around 40 K to a freezing of the delocalization of the electrons in the mixed-valence clusters.

Completely different are the spectra recorded on the highly oxidized cluster, **7**, for which a single isotropic line with g = 1.98 and ΔH_{pp} 380 G is observed between 50 and 4.2 K. The EPR spectra agree with the magnetic data and confirm that oxidation of **1a**,**b** leads to systems that have an electronic structure very similar to that of **5a**−**6**.

The main results of our studies can be summarized as follows:

(1) The $\{V_{18}O_{42}\}$ shell exists with quite different electron populations whereby the application of EPR spectroscopy and magnetochemistry allows one even to distinguish sensitively between rather small different electron populations.

(2) The $\{V_{18}O_{42}\}$ system principally shows a type of container property for different species below a critical size like e.g. H_2O, halides, formate, or nitrite.[35] The type of encapsulation of guest species can depend on the pH value. In a highly basic medium (pH 14) only a H_2O molecule is enclosed in the $\{V_{18}O_{42}\}$ shell, whereas at lower pH values *anionic species* are preferentially encapsulated. This can be attributed to the fact that protonation with concomitant decrease of the negative charge of the cluster shells reduces the repulsion between the cluster shell and the anion.

Acknowledgments. We thank the Deutsche Forschungsgemeinschaft and the Fonds der Chemischen Industrie for financial support and Prof. Dr. B. Krebs, Münster, Germany, for information regarding the isolation of a cluster compound with an encapsulated "sulfide ion".

Supporting Information Available: Tables of molar magnetic susceptibility vs temperature data (38 pages). Listings of complete structural data (CIF format) are available. Ordering and access information is given on any current masthead page.

IC9703641

(34) The oxidation of **1b** seems to be slower as EPR spectra still change through the exposition of the sample to air for about 1 week.

(35) Cram, D. J.; Cram, J. M. *Container Molecules and Their Guests*; Royal Society of Chemistry: Cambridge, U. K., 1994.